

Research Article

Look-Ahead Algorithm with Whole S-Curve Acceleration and Deceleration

Youdong Chen, Xudong Ji, Yong Tao, and Hongxing Wei

School of Mechanical Engineering and Automation, Beihang University, Beijing 100191, China

Correspondence should be addressed to Youdong Chen; chenyd@buaa.edu.cn

Received 5 April 2013; Accepted 12 May 2013

Academic Editor: Shao Zili

Copyright © 2013 Youdong Chen et al. This is an open access article distributed under the Creative Commons Attribution License, which permits unrestricted use, distribution, and reproduction in any medium, provided the original work is properly cited.

Tool paths of a complex contour machining generated by commercial CAD/CAM systems are mainly composed of many short linear/circular blocks. Though the look-ahead algorithms can improve speed and accuracy in the machining of short linear/circular segments, most of them just deal with linear segments with trapezoid acceleration and deceleration (acc/dec). In addition, the look-ahead algorithms with S-curve acc/dec are too complex to adopt the equivalent S-curve profile by approximation algorithm. To increase the smoothness of feedrate profile and machining efficiency of continuous short line and circle machining, this paper presents a feedrate profile generation approach and corresponding look-ahead algorithm with whole S-curve acc/dec. With the proposed look-ahead scheme, the feedrate profiles with S-curve acc/dec can work efficiently in a lot of short line and circle segments. Thus, the machining productivity can be increased and the feedrate profiles are smooth. The simulation and experiments verify the feasibility and validity of the proposed approach.

1. Introduction

Tool paths are currently generated by commercial CAD/CAM systems. Curves are usually approximated to a number of linear/circular blocks in CAD/CAM systems according to the feedrate and accuracy in CNC machining. During high-speed machining, the rapid and abrupt change of direction at the corner between two adjacent blocks causes vibration which is harmful to the machine mechanics and the surface finish. Therefore, to maintain the machining quality, the feedrate at the corner is set to zero in conventional NC machining, which may lead to low efficiency.

To maintain the machining quality and improve the efficiency with multiple paths within machining parameter constraints, many approaches have been proposed. One of approaches is parametric interpolation algorithms [1, 2], which generates a curved cutter path directly without segmentation contour processing. However, the computation load is heavy and inevitable errors are introduced by employing a truncated Taylor series. At the same time, there are a lot of actual workpieces described by the linear and circular codes. Therefore, there is a need to research the linear and circular interpolation algorithm.

One of the most efficient approaches is look-ahead interpolators. In order to keep the feedrate continuity, it looks ahead several paths to detect the sharp corners of paths and overrides the feedrate profile instead of planning the individual path with an acc/dec profile. References [3–7] proposed an approximation method which fit continuous short line blocks into parametric curves before interpolation. Feedrate fluctuations associated with the approximation errors should be limited in this method. Zhang et al. [8] presented a multiperiod turning method to improve the feedrate at the junctions using the linear acceleration and deceleration mode. But this method is only applied to micro line segment. Some velocity planning approaches have been proposed in [9–12]. All these methods used linear acc/dec algorithm, which usually exhibits a jump in acceleration at the beginning and the end of velocity adaptation phase. S-curve acc/dec with better servo instantaneous characteristic is used in look-ahead algorithm [13, 14]. However, it is too complex to adopt the equivalent S-curve profile by approximation algorithm. It is not a whole S-curve profile, which may lead to overshoot for large acceleration.

It should be noted that the path lengths are arbitrary in the usual NC programming. All these look-ahead algorithms

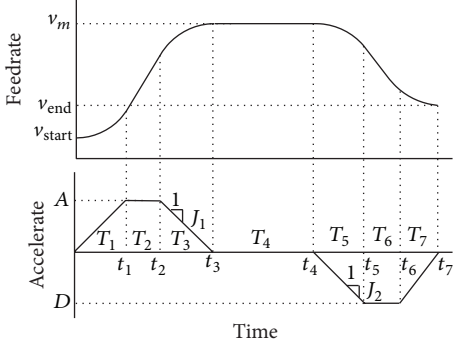


FIGURE 1: S-curve feedrate profile.

mentioned are only used for continuously microline segments. This paper proposed a look-ahead interpolation algorithm with the S-curve acc/dec for continuous linear/circular segments. During the motion, the feedrate profiles are constructed and checked within the machining constraints and the discretization of path with S-curve acc/dec. In addition, the paths of arbitrary length are also considered during interpolation.

This paper is organized as follows. In the next section, feedrate profile formulations with S-curve acc/dec are derived. Section 3 details the look-ahead algorithm. Simulation and experiments with the proposed look-ahead scheme are given in Section 4. Finally, a conclusion is given in Section 5.

2. Feedrate Profile Formulation

2.1. Discretizing the Normal S-Curve acc/dec. S-curve acc/dec can avoid mechanical shock imposed on the servo system and get stable motion along the tool path. Figure 1 shows the kinematics profiles used in the normal S-curve acc/dec. The profiles can be divided into acceleration-speed zone, constant-speed zone, and deceleration-speed zone. For the motion along the tool path, accelerations have trapezoidal profiles with prespecified slopes values. The maximum allowable acceleration and deceleration are A and D , respectively.

Considering Figure 1, the starting point feedrate is v_{start} , the end point feedrate is v_{end} , the desired feedrate is v_m , the starting and end point acceleration is zero, the maximum allowable jerk at acceleration-speed zone is J_1 , and the maximum allowable jerk at deceleration-speed zone is J_2 . The normal S-curve acc/dec has seven regions with time T_i ($i = 1, 2, \dots, 7$), $T_1 = T_3 = n_a T_s$, $T_5 = T_7 = n_b T_s$; $T_4 = n_c T_s$, $T_1/T_2 = T_5/T_6 = k$, n_a, n_b, n_c and k are integral, and T_s is the sample period. The travel length is L . If the feedrate profile is symmetrically smooth, n_a is equal to n_b . In the traditional CNC system, the times T_1, T_5 and k are prespecified. If there is acceleration or deceleration, the acceleration time or deceleration time are the prespecified constants, which may reduce efficiency. The accelerations A and D and the jerks J_1 and J_2 are prespecified in terms of machine mechanics.

2.1.1. Determination of the Numbers of Interpolation Steps for Each Region. At the acceleration zone, the desired feedrate v_m is obtained as follows:

$$v_m = v_{start} + (1 + k) J_1 T_s^2 n_a^2. \quad (1)$$

By imposing the jerk limits values on J_1 and maximum allowable acceleration A , n_a is obtained as follows:

$$n_a = \left[\sqrt{\frac{v_m - v_{start}}{(1 + k) J_1 T_s^2}} + 1 \right], \quad n_a \geq \frac{A}{J_1 T_s}. \quad (2)$$

If there is $n_a < A/J_1 T_s$, we can modify k to make $n_a \geq A/J_1 T_s$; That is,

$$k_1 = \left[\frac{J_1 (v_m - v_{start})}{A^2} - 2 \right]. \quad (3)$$

Similarly, at deceleration zone, n_b can be obtained as follows:

$$v_m = v_{end} + (1 + k) J_2 T_s^2 n_b^2, \quad (4)$$

$$n_b = \left[\sqrt{\frac{v_m - v_{end}}{(1 + k) J_2 T_s^2}} + 1 \right], \quad n_b \geq \frac{D}{J_2 T_s}. \quad (5)$$

If $n_b < D/J_2 T_s$, then

$$k_2 = \left[\frac{J_2 (v_m - v_{end})}{D^2} - 2 \right], \quad (6)$$

$$k = \min(k_1, k_2). \quad (7)$$

n_a and n_b can be obtained by (2) and (5), respectively. If k is changed, n_a and n_b are calculated by k determined by (7).

Given the numbers of interpolation steps for all regions (except the constant-speed region) specified, the travel length L is obtained as follows:

$$2L = (2 + k)((v_{start} + v_m)n_a + (v_{end} + v_m)n_b)T_s + 2v_m n_c T_s. \quad (8)$$

Then the number of interpolation step n_c for constant-speed region is calculated as follows:

$$n_c = \left[\frac{2L - (2 + k)((v_{start} + v_m)n_a + (v_{end} + v_m)n_b)T_s}{2v_m T_s} \right] + 1. \quad (9)$$

The numbers of interpolation steps for different regions are expressed as

$$\begin{aligned} N_1 &= n_a, & N_2 &= kn_a, & N_3 &= n_a, & N_4 &= n_c, \\ N_5 &= n_b, & N_6 &= kn_b, & N_7 &= n_b. \end{aligned} \quad (10)$$

n_c is rounding. There are three ways to eliminate rounding error. One is to change the desired feedrate v_m . The other is to alter starting point feedrate v_{start} . The third is to modify the end point feedrate v_{end} .

2.1.2. Modifying the Desired Feedrate. If the feedrate v_m is modified to v'_m , it can be obtained from (8), as follows:

$$v'_m = \frac{2L - (2+k)(n_a v_{\text{start}} + n_b v_{\text{end}}) T_s}{(2n_c + (2+k)(n_a + n_b)) T_s}. \quad (11)$$

The jerk at acceleration-speed zone can be recalculated from (1):

$$J'_1 = \frac{v'_m - v_{\text{start}}}{(1+k)n_a^2 T_s^2}. \quad (12)$$

Similarly, the jerk at deceleration-speed zone can be recomputed as follows:

$$J'_2 = \frac{v'_m - v_{\text{end}}}{(1+k)n_b^2 T_s^2}. \quad (13)$$

The readjusted values of jerks and feedrate should not be greater than the maximum allowable values. Considering (9), (11), (12), and (13), the following in-equations are valid:

$$J'_1 \leq J_1, \quad J'_2 \leq J_2, \quad v'_m \leq v_m. \quad (14)$$

For the machining, the feedrate cannot be changed too drastically. Therefore, it is necessary to check the feedrate variation η :

$$\eta = \left| \frac{v_m - v'_m}{v_m} \right|. \quad (15)$$

Then we can arrived at

$$\eta < \frac{1}{n_a + n_b + n_c}. \quad (16)$$

For normal block, the value of $n_a + n_b + n_c$ is much greater than 1, so that the feedrate variation can be neglected.

The S-curve acc/dec sampled-data formulation for each region can be determined by the method stated in [15]. It is

$$f(t) = \begin{cases} v_{\text{start}} + pJ'_1(3n^2 + 3n + 1), & 0 \leq n < n_a, \\ v_{\text{start}} + 3pJ'_1 n_a (2n_2 + n_a + 1), & 0 \leq n_2 < kn_a, \\ v_{\text{start}} + pJ'_1 (3n_a^2 + 6kn_a^2 + 6n_a n_3 - 3n_3^2 - 3n_3 - 1), & 0 \leq n_3 < n_a, \\ v'_m, & 0 \leq n_4 < n_c, \\ v_{\text{end}} + pJ'_2 ((6+k)n_b^2 - 3(n_5 - (k+2)n_a)^2 - 3(n_5 - (k+2)n_a) - 1), & 0 \leq n_5 < n_b, \\ v_{\text{end}} + 3pJ'_2 n_b (n_a + 2n_b - 2n_6 - 1), & 0 \leq n_6 < kn_b, \\ v_{\text{end}} + pJ'_2 (3n_b^2 - 6n_b n_7 - 3n_b + 3n_7^2 + 3n_7 + 1), & 0 \leq n_7 < n_b, \end{cases} \quad (17)$$

where

$$\begin{aligned} p &= \frac{1}{6} T_s^2, & n_2 &= n - n_a, & n_3 &= n - (k+1)n_a, \\ n_4 &= n - (k+2)n_a, & n_5 &= n - (k+2)n_a - n_c, & n_6 &= n - (k+2)n_a - n_c - n_b, \\ n_7 &= n - (k+2)n_a - n_c - (k+1)n_b. \end{aligned} \quad (18)$$

2.1.3. Altering the Starting Point Feedrate. If the starting point feedrate is changed, n_c is obtained as follows:

$$n_c = \left[\frac{2L - (2+k)((v_{\text{start}} + v_m)n_a + (v_{\text{end}} + v_m)n_b)T_s}{2v_m T_s} \right]. \quad (19)$$

The starting point feedrate can be calculated from (8) as follows:

$$v'_{\text{start}} = \frac{(v_{\text{end}} + v_m)n_b}{n_a} + \frac{2L - 2v_m n_c T_s}{(2+k)n_a T_s} - v_m. \quad (20)$$

The jerk at acceleration-speed zone can be recomputed from (1):

$$J'_1 = \frac{v_m - v'_{\text{start}}}{(1+k)n_a^2 T_s^2}. \quad (21)$$

The sampled-data formulations of S-curve acc/dec for each region are similar to (13). Considering (19), (20), and (21), there is a relationship as follows:

$$J'_1 \leq J_1, \quad v'_m = v_m, \quad v'_{\text{start}} \geq v_{\text{start}}. \quad (22)$$

2.1.4. Readjusting the End Point Feedrate. If the end point feedrate is modified, n_c is obtained from (19). The end point feedrate is recalculated from (8) as follows:

$$v'_{\text{end}} = \frac{2L - 2v_m n_c T_s}{(2+k)n_b T_s} + \frac{(v_{\text{start}} + v_m)n_a}{n_b} - v_m. \quad (23)$$

The jerk at deceleration-speed zone can be derived from (3):

$$J'_2 = \frac{v_m - v'_{\text{end}}}{(1+k)n_b^2 T_s^2}. \quad (24)$$

The sampled-data formulations of S-curve acc/dec for each region are similar to (13). Considering (19), (23), and (24), we can reach

$$J'_2 \leq J_2, \quad v'_m = v_m, \quad v'_{\text{end}} \geq v_{\text{end}}. \quad (25)$$

We can adjust v_{start} , v_{end} , v_m , J_1 , or J_2 to discretizing linear/circular path with S-curve acc/dec. This provides a way of calculating the trajectory machining parameters for look-ahead interpolation.

2.2. Feedrate and Travel Length Constraints. In order to generate a feedrate profile, it is necessary to check the path which is a normal or short block. The normal block has acceleration-speed zone, constant-speed zone, and deceleration-speed zone, shown in Figure 1. The short block does not have constant-speed zone. The S-curve acc/dec sampled-data formulations of normal block are (17). The formulations of short block are similar to (17). According to the travel length, the path is divided into seven types. The normal block refers to Type 1. Types 2 to 7 belong to the short block. Type 1 should satisfy

$$L \geq 0.5(2+k)((v_{\text{start}} + v_m)n_a + (v_{\text{end}} + v_m)n_b)T_s. \quad (26)$$

Type 2 which has no constant-speed zone (that means n_c is zero) is shown in Figure 2(a). It has an acceleration-speed zone and a deceleration-speed zone with constant-acceleration regions. It accelerates to a certain speed from starting point feedrate, then changes to deceleration-speed zone and reaches the end point at feedrate v_{end} . With the travel length shortening, the time of constant-acceleration region is decreasing. In case of Type 2, the following equation should be satisfied:

$$\begin{aligned} L &< 0.5(2+k)((v_{\text{start}} + v_m)n_a + (v_{\text{end}} + v_m)n_b)T_s, \\ L &\geq ((v_{\text{start}} + v_m)n_a + (v_{\text{end}} + v_m)n_b)T_s. \end{aligned} \quad (27)$$

Type 3 has neither constant-speed zone nor constant-acceleration regions (that means n_b and n_c are zero), as shown in Figure 2(b). Type 3 also has acceleration-speed zone and deceleration-speed zone. The difference between Type 3 and Type 2 is that Type 3 has no constant-acceleration regions. The condition in Type 3 is represented as follows:

$$\begin{aligned} v_{\text{start}} &< v_{\text{end}} < v_m, \\ L &< ((v_{\text{start}} + v_m)n_a + (v_{\text{end}} + v_m)n_b)T_s, \end{aligned} \quad (28)$$

$$2L \geq ((2+k)n_a(v_{\text{start}} + v_m))T_s$$

or

$$\begin{aligned} v_{\text{end}} &< v_{\text{start}} < v_m, \\ L &< ((v_{\text{start}} + v_m)n_a + (v_{\text{end}} + v_m)n_b)T_s, \quad (29) \\ 2L &\geq ((2+k)n_b(v_{\text{start}} + v_m))T_s. \end{aligned}$$

In case end point feedrate is equal to v_m , Type 4 that has constant-speed and acceleration-speed zones is to accelerate to speed v_m and keeps moving at this speed until end point is reached. Or if starting point feedrate is equal to v_m , Type 4 that has constant-speed and deceleration-speed zones keeps moving at speed v_m until the deceleration point is reached;

then the speed decelerates to v_{end} . Equation (29) needs to be satisfied for Type 4, as shown in Figure 2(c):

$$\begin{aligned} v_{\text{start}} &< v_{\text{end}} = v_m, \\ 2L &\geq (2+k)n_a(v_{\text{start}} + v_{\text{end}})T_s \\ \text{or} \\ v_{\text{end}} &< v_{\text{start}} = v_m, \\ 2L &\geq (2+k)n_b(v_{\text{start}} + v_{\text{end}})T_s. \end{aligned} \quad (30)$$

The difference between Type 5 and Type 4 is that the starting and end point feedrates of Type 5 are not equal to v_m , as shown in Figure 2(d). If end point feedrate v_{end} is greater than starting point feedrate v_{start} , Type 5 accelerates to end point feedrate v_{end} from starting point feedrate v_{start} . If end point feedrate v_{end} is less than starting point feedrate v_{start} , Type 5 decelerates to end point feedrate v_{end} from v_{start} . In case of Type 5, (30) should be satisfied:

$$\begin{aligned} v_{\text{start}} &< v_{\text{end}} < v_m, \\ 2L &< (2+k)n_a(v_{\text{start}} + v_m)T_s, \\ L &\geq n_a(v_{\text{start}} + v_{\text{end}})T_s \\ \text{or} \\ v_{\text{end}} &< v_{\text{start}} < v_m, \\ 2L &< (2+k)n_a(v_{\text{start}} + v_m)T_s, \\ L &\geq n_b(v_{\text{start}} + v_{\text{end}})T_s. \end{aligned} \quad (31)$$

Without constant-acceleration region, Type 6 has only acceleration-speed or deceleration-speed zone, shown in Figure 2(e). It is checked as

$$\begin{aligned} v_{\text{start}} &< v_{\text{end}} \leq v_m, \\ L &< n_a(v_{\text{start}} + v_{\text{end}})T_s, \\ L &\geq (v_{\text{start}} + v_{\text{end}})T_s \\ \text{or} \\ v_{\text{end}} &< v_{\text{start}} \leq v_m, \\ L &< n_b(v_{\text{start}} + v_{\text{end}})T_s, \\ L &\geq (v_{\text{start}} + v_{\text{end}})T_s. \end{aligned} \quad (32)$$

If the travel length is short enough, the type of S-curve acc/dec refers to Type 7, shown in Figure 2(f). Starting with

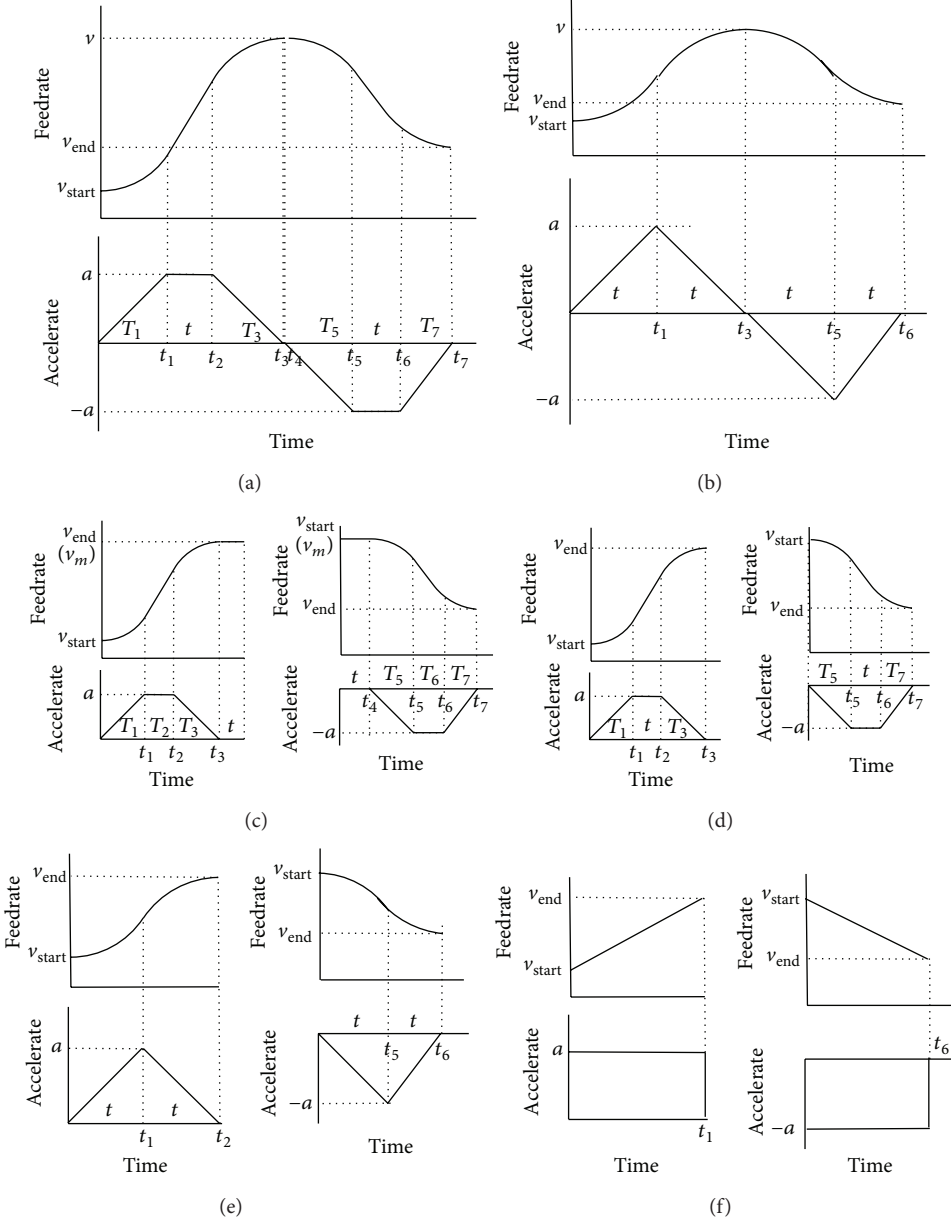


FIGURE 2: Various kinematics profiles for movement of specified travel length.

v_{start} , Type 7 accelerates or decelerates to v_{end} at the end point. Type 7 is tested as

$$\begin{aligned} v_{\text{start}} &< v_{\text{end}} \leq v_m, \\ L &< (v_{\text{start}} + v_{\text{end}}) T_s \\ \text{or} \\ v_{\text{end}} &< v_{\text{start}} \leq v_m, \\ L &< (v_{\text{start}} + v_{\text{end}}) T_s. \end{aligned} \quad (33)$$

2.3. Corner Angle Constraints. The feedrate and its direction could be changed at the path turning point, which may cause acceleration. The acceleration that should be less than the

maximum allowable acceleration a_{\max} is associated with the turning angle α and the feedrate v_t at the corner point. v_t should meet the following [11]:

$$v_t \leq \frac{a_{\max} \cdot T_s}{2 \sin(\alpha/2)}, \quad (34)$$

$$v = \min(v_t, v_m). \quad (35)$$

The corner angle is the angle between the path tangent τ_i of forward direction and the next path tangent τ_{i+1} at the turning point, shown in Figure 3. There are four different types at the turning point: line to line, line to arc, arc to line,

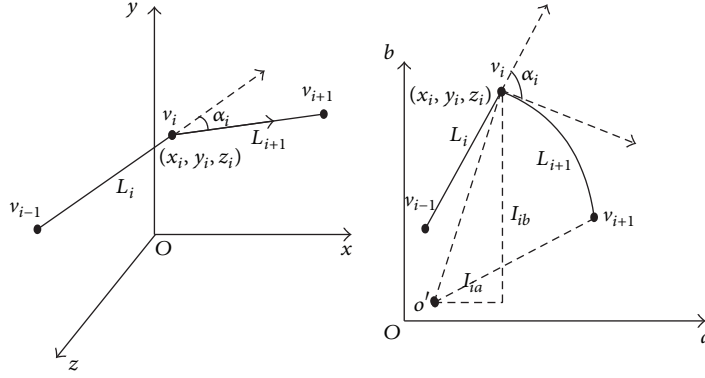


FIGURE 3: The turning angle.

and arc to arc. The corner angle α between two consecutive path segments is given as

$$\cos \alpha = \frac{\tau_i \cdot \tau_{i+1}}{|\tau_i| |\tau_{i+1}|}. \quad (36)$$

3. Look-Ahead Scheme

The look-ahead algorithm which takes the characteristics of path, machine tool, and feedrate profile into consideration realizes the smooth transfer in interpath. The look-ahead scheme assures the smooth movement and the accessibility of the starting point and end point feedrates of each path.

The interpolation of G01, G02, and G03 codes can be achieved by adjusting starting point feedrate v_{start} , end point feedrate v_{end} , and feedrate v_m according to the travel length and the machining parameters. There are three types of algorithm to adjust machining parameters.

Algorithm A. The interpolation can be achieved by modifying the starting point feedrate v_{start} and jerk J_1 .

Algorithm B. The interpolation can be completed by adjusting the end point feedrate v_{end} and jerk J_2 .

Algorithm C. The interpolation can be realized by recalculating the feedrate v_m and jerks J_1, J_2 , but the starting point and end point feedrates are not changed.

3.1. Algorithm of Look-Ahead Scheme. In order to guarantee the accessibility of the starting point and end point feedrates of each path, the look-ahead scheme is realized as follows.

Step 1 (calculating turning point feedrates). The controller reads j paths before interpolation and the look-ahead path number j is determined by the controller. The starting point feedrate of the first path and the end point feedrate of last path are v_{start}^0 and v_{end}^0 , respectively. The feedrates at turning point are obtained by (35).

Step 2 (dividing the paths into blocks). Starting with the first path, the end point feedrates of each path are determined by Algorithm B in order until the last path. The break paths are

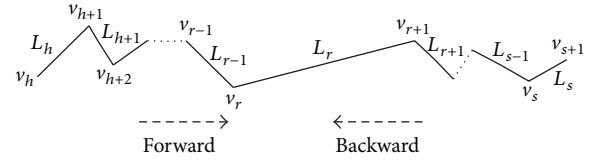


FIGURE 4: The look-ahead path.

checked and recorded. The break path whose travel length is so short that the path cannot be interpolated with the S-curve acc/dec is referred to as Type 7. The starting point and end point feedrates of the break path are set according to Type 7.

The paths are divided into blocks by break paths. All the paths lying in every two adjacent break paths are classified into one block. The starting point feedrate of the block is the end point feedrate of the front break path. The end point feedrate of the block is the starting point feedrate of the behind break path.

The longest perfect paths of each block are checked and recorded. The perfect path that can be determined by Algorithm C is referred to as the path in which the interpolation can be completed by adjusting feedrate v_m and jerks J_1, J_2 ; the starting and end point feedrates are not changed. Types 1 to 6 belong to the perfect path.

Step 3 (determine the starting and end point feedrates). Supposing paths L_h, L_{h-1}, \dots, L_s belong to a block, L_r is the longest perfect path, shown in Figure 4. Starting with the path L_h , the end point feedrates v_g ($g = h+1, h+2, h+3, \dots, r-1, r$) of paths are determined by Algorithm B in order until the path L_{r-1} . The end point feedrate of path L_{r-1} and the starting point feedrate of the path L_r are v_r . Starting with L_s , the starting point feedrate v_w ($w = s+1, s, \dots, r+1$) of path is determined by Algorithm A in the reverse order until the path L_{r+1} . The starting point feedrate of path L_{r+1} and the end point feedrate of path L_r are v_{r+1} . The starting point and end point feedrates of the longest perfect path L_r are v_r and v_{r+1} , respectively. Since L_r is perfect path, it can be interpolated by recalculating the feedrate v_m and jerks J_1, J_2 , the starting point and end point feedrates are not changed. Step 3 is repeated until all the blocks are treated and all the starting and end

TABLE 1: Coordinates of path to be machined (mm).

Number	Type	Coordinate value	Center of arc	Number	Type	Coordinate value	Center of arc
0		(2.16, 10.672)					
1	Line	(3.952, 11.016)		6	Circle	(12.416, 8.4)	(11.432, 87.649)
2	Line	(5.768, 11.064)		7	Line	(18.552, 11.016)	
3	Line	(7.568, 10.808)		8	Line	(19.696, 4.48)	
4	Line	(9.312, 10.272)		9	Line	(20.936, 5.776)	
5	Line	(10.936, 9.46)		10	Line	(22.256, 5.232)	

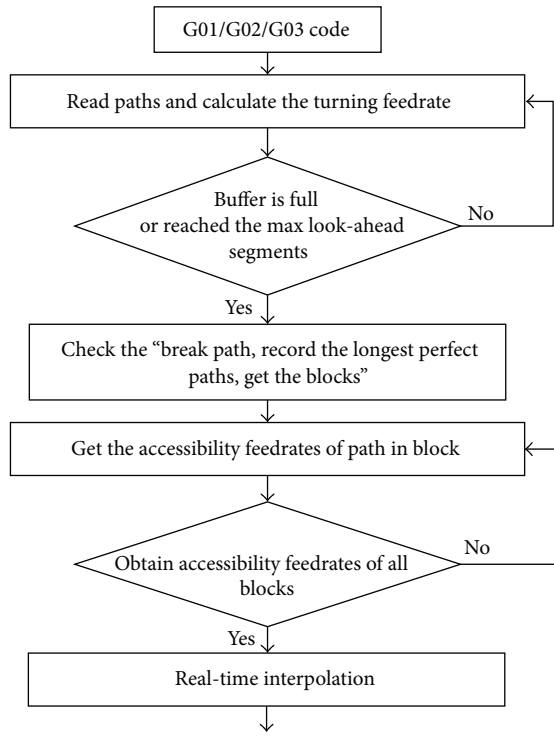


FIGURE 5: Flowchart of look-ahead scheme.

point feedrates of paths are recorded in the look-ahead buffer queue.

Step 4 (real-time interpolation). Take the first path in the look-ahead buffer queue. Calculate the time of every region with the S-curve acc/dec and compute the interpolation point in S-curve acc/dec sampled-data formulations. The movements of mechanics are executed according to the interpolation points. When the interpolation of current line is completed, *Step 4* is repeated until all the paths are finished. The look-ahead scheme flowchart is shown in Figure 5.

4. Simulation and Experiment

Several simulations and experiments applying the proposed approach were made on a CNC milling machine, in which

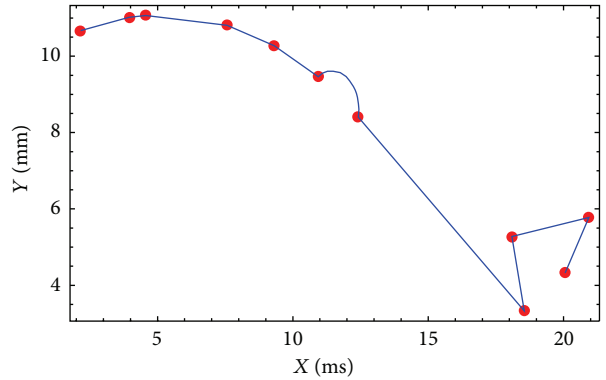


FIGURE 6: The tool paths of the look-ahead scheme.

$$v_m = 2 \text{ m/min}, A = D = 40 \text{ m/s}^2, J_1 = J_2 = 10 \text{ m/s}^3, \text{ and } T_s = 1 \text{ ms}.$$

Table 1 shows the coordinates of the starting and end points of 10 small linear/circular segments describing a piece of 2D curve which is deliberately chosen to test the proposed look-ahead scheme. As shown in Figure 6, the first five paths are lines. The sixth path is a circle. There are two sharp corners from the seventh to the tenth path.

The feedrate profiles are shown in Figure 7. Without look-ahead scheme, it has always the acceleration and deceleration phases in each path and the machine tool never reaches the desired feedrate, as shown in Figure 7(a). With the proposed look-ahead scheme, although there are two sharp corners, the feedrate accelerates to desired feedrate and almost keeps moving in this speed until the end point, as shown in Figure 7(b).

The proposed look-ahead scheme can decrease the numbers of the break paths and zero feedrate. As shown in the first row of Table 2, the travel length of path 2 is too short. In [12–14], path 2 is a break path whose starting and end point feedrates are zero.

With this look-ahead scheme, path 2 is not a break path, as shown in Table 2. As shown in Figure 5, there are two sharp corners at the turning points of point 8 and 10. In [12–14], the end point feedrates of seventh and ninth path segment are zero. With this proposed look-ahead scheme, the end point feedrates of seventh and ninth path segment are not zero, as shown in Table 2. As a result, the machining time with the proposed look-ahead scheme was approximately 1 s, while the

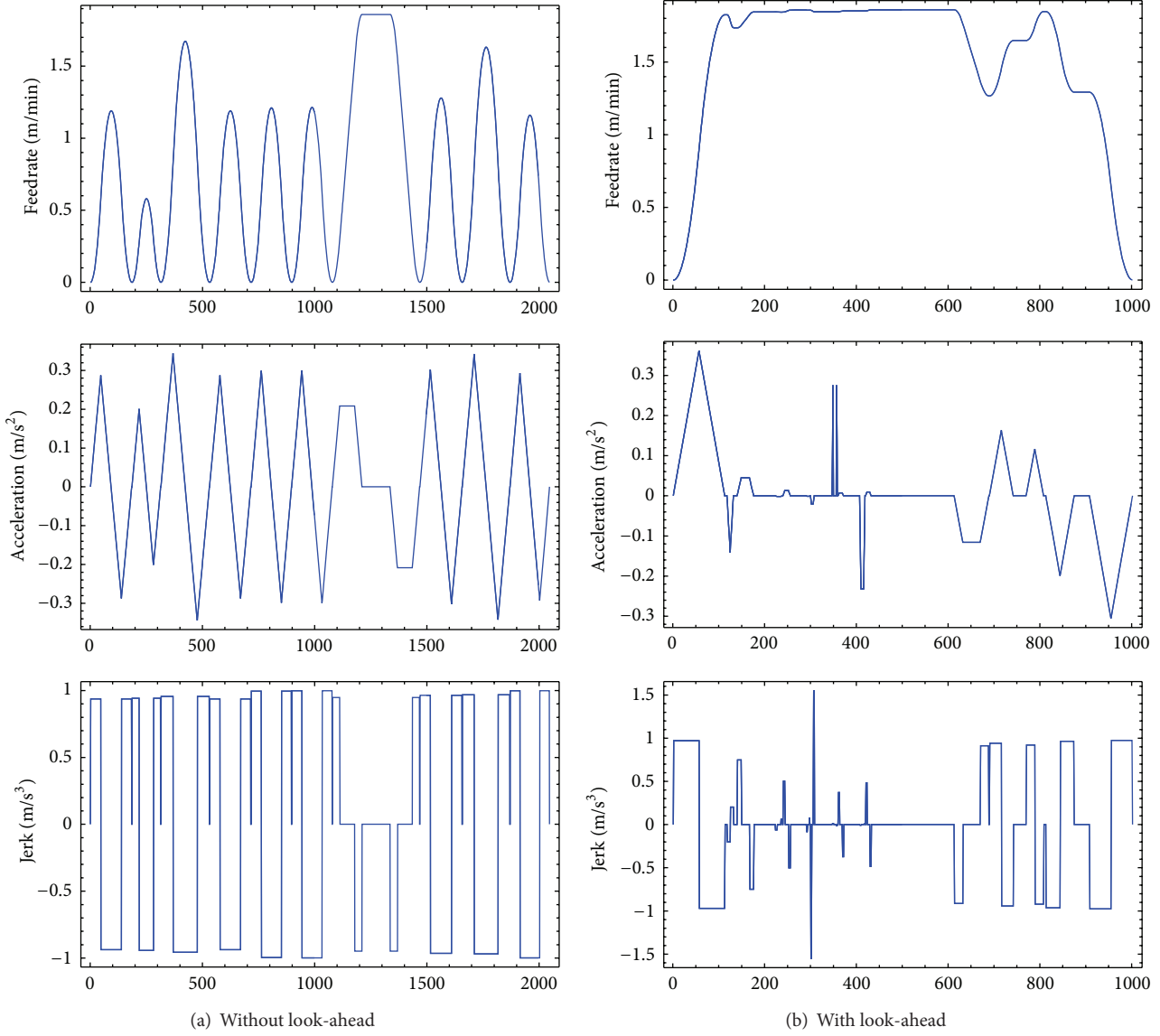


FIGURE 7: Feedrate profiles of S-curve acc/dec characteristics without/with look-ahead.

TABLE 2: The end point feedrate (m/min) and travel length (mm).

Number	1	2	3	4	5	6	7	8	9	10
End feedrate	1.82	1.74	1.84	1.86	1.85	1.85	1.27	1.65	1.29	0
Travel length	1.825	0.617	3.011	1.825	1.816	1.82	7.96	2.0	2.883	1.701

time without the look-ahead scheme was about 2 s, as shown in Figure 7.

The part shown in Figure 8 was machined on a five-axis machining center controller with an in-house developed CNC running on microC/OS-II real-time operation system. The experimental results showed that the machining time was dramatically shortened when the proposed approach is

applied. Moreover, the feedrates are smoother than those without look-ahead approach and the final contour accuracy of the parts is satisfying.

5. Conclusion

Look-ahead scheme is the key issue of high speed and high precision CNC machining for small paths. We propose a feedrate profile generation approach and corresponding look-ahead algorithm with whole S-curve acc/dec. The proposed look-ahead scheme can handle both small line and circle segments. The feedrate profiles generation effectively predetermines the numbers of interpolation steps for different regions and the discretion feedrate of the path with S-curve acceleration and deceleration. As a result, the look-ahead algorithms with S-curve acceleration and deceleration easily meet real-time requirements. The simulations and

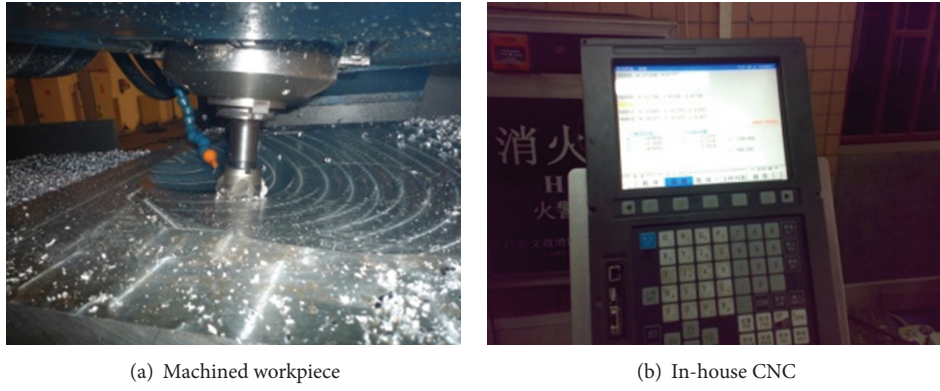


FIGURE 8: A machined workpiece with the developed look-ahead approach.

experiments showed that the proposed approach is feasible and effective.

Acknowledgments

The work presented in this paper was supported by the Major National S&T Program of China (Grant no. 2011ZX04002-151) and National 863 Program (Grant no. 2011AA04A104).

References

- experiments showed that the proposed approach is feasible and effective.

Acknowledgments

The work presented in this paper was supported by the Major National S&T Program of China (Grant no. 2011ZX04002-151) and National 863 Program (Grant no. 2011AA04A104).

References

 - [1] D. C. H. Yang and T. Kong, "Parametric interpolator versus linear interpolator for precision CNC machining," *Computer-Aided Design*, vol. 26, no. 3, pp. 225–234, 1994.
 - [2] M. Shpitalni, Y. Koren, and C. C. Lo, "Realtime curve interpolators," *Computer-Aided Design*, vol. 26, no. 11, pp. 832–838, 1994.
 - [3] H. Yau and M. Kuo, "NURBS machining and feed rate adjustment for high-speed cutting of complex sculptured surfaces," *International Journal of Production Research*, vol. 39, no. 1, pp. 21–41, 2001.
 - [4] M. Zhang, W. Yan, C. Yuan, D. Wang, and X. Gao, "Curve fitting and optimal interpolation on CNC machines based on quadratic B-splines," *Science China Information Sciences*, vol. 53, no. 1, pp. 1–12, 2010.
 - [5] H.-T. Yau and J.-B. Wang, "Fast Bezier interpolator with real-time lookahead function for high-accuracy machining," *International Journal of Machine Tools and Manufacture*, vol. 47, no. 10, pp. 1518–1529, 2007.
 - [6] J. B. Wang and H. T. Yau, "Real-time NURBS interpolator: application to short linear segments," *International Journal of Advanced Manufacturing Technology*, vol. 41, no. 11–12, pp. 1169–1185, 2009.
 - [7] J. A. Tao, S. L. Gao, Q. N. You, and Q. Shi, "Lookahead and acceleration/deceleration algorithms for micro-line blocks machining," *Journal of Computer-Aided Design and Computer Graphics*, vol. 22, no. 9, pp. 1570–1586, 2010.
 - [8] L. X. Zhang, R. Y. Sun, X. S. Gao, and H. B. Li, "High speed interpolation for micro-line trajectory and adaptive real-time lookahead scheme in CNC machining," *Science China Technological Sciences*, vol. 54, no. 6, pp. 1481–1495, 2011.
 - [9] L. B. Zhang, Y. P. You, J. He, and X. F. Yang, "The transition algorithm based on parametric spline curve for high-speed machining of continuous short line segments," *International Journal of Advanced Manufacturing Technology*, vol. 52, no. 1–4, pp. 245–254, 2011.
 - [10] C. Lee, "Generation of velocity profiles with speed limit of each axis for high-speed machining using look-ahead buffer," *International Journal of Precision Engineering and Manufacturing*, vol. 11, no. 2, pp. 201–208, 2010.
 - [11] J. Hu, L. Xiao, Y. Wang, and Z. Wu, "An optimal feedrate model and solution algorithm for a high-speed machine of small line blocks with look-ahead," *International Journal of Advanced Manufacturing Technology*, vol. 28, no. 9, pp. 930–935, 2006.
 - [12] Y. Wang, L. Xiao, S. Zeng, Z. Wu, and S. Zhong, "Optimal feedrate model and solution for high-speed machining of small line blocks with look-ahead," *Journal of Shanghai Jiaotong University*, vol. 38, no. 6, pp. 901–904, 2004.
 - [13] J. He, Y. You, H. Chen, and H. Wang, "A fast nested lookahead algorithm with S-shape acceleration and deceleration," *Acta Aeronautica et Astronautica Sinica*, vol. 31, no. 4, pp. 842–851, 2010.
 - [14] Y. N. Cao, T. M. Wang, Y. D. Chen, and H. X. Wei, "Application of pre-interpolation S-shape acceleration/deceleration in CNC look-ahead interpolation algorithm," *Journal of Beijing University of Aeronautics and Astronautics*, vol. 33, no. 5, pp. 594–599, 2007.
 - [15] Y. Chen, H. Wei, K. Sun, M. Liu, and T. Wang, "Algorithm for smooth S-curve feedrate profiling generation," *Chinese Journal of Mechanical Engineering*, vol. 24, no. 2, pp. 237–247, 2011.